Rituximab inhibits B-cell receptor signaling

Samar Kheirallah,[1,2] Pierre Caron,[1,2] Emilie Gross,[1,2] Anne Quillet-Mary,[1,2] Justine Bertrand-Michel,[3] Jean-Jacques Fournié,[1,2] Guy Laurent,[1,2,4] and Christine Bezombes[2]

[1]Inserm, U563, Toulouse; [2]Université Toulouse III Paul-Sabatier, Centre de Physiopathologie de Toulouse Purpan, Toulouse; [3]Plateau de lipidomique, Institut Fédératif de Recherche (IFR) 150, Inserm, Toulouse; and [4]Centre Hospitalier Universitaire (CHU) Toulouse, Hôpital Purpan, Service Hématologie, Toulouse, France

Rituximab (RTX), a monoclonal antibody directed against the CD20 protein, is a drug commonly used in the treatment of B-cell–derived lymphoid neoplasias and of antibody-mediated autoimmune diseases. In addition to cell- and complement-mediated B-cell depletion, RTX is thought to inhibit B-cell survival and proliferation through negative regulation of canonical signaling pathways involving Akt, ERK, and mammalian target of rapamycin. However, surprisingly, although B-cell receptor (BCR) signaling has been considered critical for normal and more recently, for neoplastic B cells, the hypothesis that RTX could target BCR has never been investigated. Using follicular lymphoma cell lines as models, as well as normal B cells, we show here, for the first time, that pretreatment with RTX results in a time-dependent inhibition of the BCR-signaling cascade involving Lyn, Syk, PLCγ2, Akt, and ERK, and calcium mobilization. The inhibitory effect of RTX correlates with decrease of raft-associated cholesterol, complete inhibition of BCR relocalization into lipid raft microdomains, and down-regulation of BCR immunoglobulin expression. Thus, RTX-mediated alteration of BCR expression, dynamics, and signaling might contribute to the immunosuppressive activity of the drug. (Blood. 2010;115: 985-994)

Introduction

Rituximab (RTX) is a monoclonal antibody directed against the CD20 membrane-associated glycoprotein expressed on normal human B cells and most malignant B cell–derived neoplasias. RTX has been largely used, alone or in combination with chemotherapy, in the treatment of chronic lymphoid neoplasias in large cohorts of patients with significant clinical benefit, especially in follicular lymphoma (FL) and diffuse large B cell lymphoma (DLBCL).[1] RTX has also proven efficacy in autoimmune diseases, including autoimmune cytopenia and rheumatoid arthritis.[2] It is currently admitted that RTX acts through normal or malignant B-cell depletion, which operates through antibody-dependent cellular cytotoxicity, complement-mediated cell lysis, and direct inhibitory effect (cell growth inhibition or apoptosis). At the present time, the respective contribution of each of these mechanisms has not been yet fully characterized in clinical settings.[3-5] Although RTX has been used for more than a decade in more than a million patient encounters, elucidating its mechanism of action still remains an important issue.

Although compelling evidence suggests a major role for antibody-dependent cellular cytotoxicity, we and others have largely documented that RTX also triggers a complex network of direct inhibitory signals that can be divided in 3 categories. The first group consists in membrane-associated proximal events, including sphingolipid distribution alterations, modifications of lipid raft microdomains, and calcium fluxes, as well as release of potent lipidic second messengers, such as ceramide.[6-8] The second group consists of the inhibition of canonical signaling pathways involving MAPK, phosphoinositide 3-kinase/Akt, some specific protein kinase C isoforms, nuclear factor-κB, and mammalian target of rapamycin.[5,9] The last group is composed of regulation of proteins controlled by these signaling modules, Bcl-2 proteins family being the most representative.[10,11] Although all these events might interfere with B-cell proliferation and survival, RTX-mediated CD20 activation probably results in the inhibition of additional B cell–specific survival pathways. In this context, based on the role of ligand-induced B-cell receptor (BCR) activation in normal B-cell proliferation and survival, we hypothesized that RTX could interfere with BCR signaling.

BCR is a protein complex constituted by immunoglobulins (Ig), Igα (CD79a), Igβ (CD79b), the 2 latter containing immunoreceptor tyrosine-based activation motifs (ITAMs).[12] Ligand-induced BCR activation results in its oligomerization and translocation to cholesterol-enriched raft microdomains, in which Igα and Igβ are phosphorylated by Src family kinases Lyn, Fyn, and Blk.[13-15] Among these phosphorylation events, Lyn activation plays a central role because it results in the recruitment on ITAM of the nonreceptor tyrosine kinase Syk, this step being critical for the propagation of BCR signaling.[16] Syk displays an autophosphorylation site (Y525) and 2 Lyn-targeted tyrosine motifs (Y348 and Y352).[17] On Syk phosphorylation, BCR signaling propagates through downstream canonical pathways, including phospholipase C and subsequent Ca^{2+} release as well as stimulation of ERK/MAPK and Akt.[18] In addition, BCR is finely tuned through different regulators among which the tyrosine phosphatase SHP-1 plays a critical function.[19] Recent studies have identified BCR regulation disturbances in some neoplastic B cells. Indeed, Chen et al have described a constitutive high level of Syk phosphorylation at Y348/Y352 in DLBCL, supporting the concept of "tonic BCR" in this disease.[20] Irish et al have described that stimulated FL cells display greater levels of BCR-induced phosphorylation of Syk (Y352), Btk, and MAPK.[21] Thus, FL cells represent models suitable for evaluating pharmacologic targeting of BCR signaling.

Submitted August 8, 2009; accepted October 11, 2009. Prepublished online as *Blood* First Edition paper, November 17, 2009; DOI 10.1182/blood-2009-08-237537.

The publication costs of this article were defrayed in part by page charge payment. Therefore, and solely to indicate this fact, this article is hereby marked "advertisement" in accordance with 18 USC section 1734.

In this study, we hypothesized that RTX could interfere with BCR signaling, from 3 lines of evidence. First, RTX induces sharp changes in the organization of raft microdomains.[7,8] Second, treatment with RTX inhibits Lyn activity at least in B-cell lymphoma.[22] Finally, RTX is potentially active against distal signaling events, such as ERK and Akt activity.[9] This study was aimed at studying the influence of RTX on BCR signaling in FL cell lines and in normal B cells.

Methods

Cell lines and reagents

RL and DOHH2 are transformed FL cell lines carrying the t(14;18). They were obtained from ATCC and Deutsche Sammlung von Mikroorganismen und Zellkulturen, respectively. RL subclones (1G11 and 2B11) were obtained using limiting dilution assay. CD20 quantification was performed with Quantibrite kit (BD Biosciences). Cells were cultured at 37°C in 5% CO_2 in RPMI supplemented with 10% fetal calf serum (FCS), glutamine (2mM), streptomycin (10 μg/mL), and penicillin (200 U/mL; Invitrogen).

Peripheral blood mononuclear cells (PBMCs) were collected from healthy donors (Etablissement Fraçais du Sang, CHU Purpan) and separated by Ficoll-Hypaque density gradient (GE Healthcare). Cytometry analyses were performed by gating on $CD19^+$ populations.

RTX and alemtuzumab (Campath-H1) were kindly provided by Roche Pharma. Nonimmune human IgG, MG132, methyl-β-cyclodextrin (MβCD), ionomycin, filipin, and sodium orthovanadate were purchased from Sigma-Aldrich.

F(ab′)2 RTX preparation

F(ab′)2 RTX was produced according to Pierce F(ab′)2 preparation kit instructions (Perbio Sciences). Briefly, 2 mg of RTX was digested by immobilized pepsin, and F(ab′)2 was purified using immobilized protein A column and separated from Fc fragment by centrifugation on Amicon Ultra-4 filter tube (Millipore). F(ab′)2 purity was verified by migration on sodium dodecyl sulfate–polyacrylamide gel electrophoresis) and Ponceau coloration. F(ab′)2 was ultimately prepared at 10 mg/mL in phosphate-buffered saline (PBS).

BCR stimulation

Cells were seeded at 0.3 million cells/mL 24 hours before treatment. Entire RTX (for RL cells) or F(ab′)2 RTX (for normal B cells or DOHH2) was added at 10 μg/mL for 16 hours, and then cells were stimulated with F(ab′)2 goat anti–human (Fc fragment specific) IgM (RL), IgG (DOHH2), or IgM/IgG (normal B cells; Jackson ImmunoResearch Laboratories) at 10 μg/mL for the indicated times. Because DOHH2 cells trigger IgG isotype BCRs, these cells were treated with F(ab′)2 RTX to avoid human RTX Fc fragment cross-reaction with F(ab′)2 goat anti–human IgG used for BCR stimulation.

For cholesterol depletion, cells were incubated in complete medium containing 5mM MβCD during 30 minutes at 37°C before filipin staining or BCR stimulation. For proteasome inhibition, 10μM of MG132 was coincubated with 10 μg/mL of RTX during 16 hours. For tyrosine phosphatase inhibition, sodium orthovanadate was used at 0.1mM for 1 hour before RTX treatment.

Flow cytometric analysis

For intracellular protein staining, cells were washed with cold PBS, fixed for 10 minutes at room temperature with 4% paraformaldehyde (pH 7.4), and permeabilized 10 minutes at room temperature with 0.1% saponin.

BCR activation was analyzed on BDLSRII cytometer (BD Biosciences) using an anti–phospho-Syk (Y525/526) primary antibody (Cell Signaling Technology) at 0.4 μg/mL and a secondary goat anti–rabbit fluorescein isothiocyanate-conjugated antibody (Jackson ImmunoResearch Laboratories) at 5 μg/mL or a phycoerythrin-conjugated anti–phospho-Syk (Y348 or Y352; BD Biosciences). Cy5-conjugated anti-IgM or IgG antibodies (Jackson ImmunoResearch Laboratories) were used for BCR expression analyses. Cholesterol staining was performed on fixed cells using filipin at 50 μg/mL. Flow cytometric data were analyzed using FlowJo software Version 7.2.5 (TreeStar) for overlay representations and DIVA 6.1.2 (BD Biosciences) software for other interpretations.

Western blot

Analyses were performed as we previously described.[9] The different antibodies used for Western blot were as follows: anti-Akt, anti–phospho-Akt (Thr 308), anti-ERK, anti-PLCγ2, anti–phospho-PLCγ2 (Y1217), anti–phospho-tyrosine (P-Tyr-100), anti–phospho-Src (Y416; all from Cell Signaling Technology), anti-Igα, anti-Lyn (from Santa Cruz Biotechnology), anti–phospho-ERK (T183, Y185; Sigma-Aldrich), anti–β-actin (Lab Vision), goat anti–human IgG, or IgM Fc fragment-specific (Jackson ImmunoResearch Laboratories). Horseradish peroxidase–conjugated secondary antibodies against rabbit, mouse, or goat immunoglobulins were from Jackson ImmunoResearch Laboratories.

Immunoprecipitation

After F(ab′)2 RTX treatment, 5×10^6 cells were washed with PBS and lysed with RadioImmuno Precipitation Assay (RIPA) buffer (20mM Tris, pH 7.4, 150mM NaCl, 4mM ethylenediaminetetraacetic acid, and 0.5% Triton X-100) supplemented with protease inhibitor cocktail (Sigma-Aldrich). Cell lysates were sonicated and centrifuged 10 minutes at 13 000*g* at 4°C. The supernatant was precleared during 1 hour with 25 μL of protein A-Sepharose beads (GE Healthcare). After preclearing, 500 μg of supernatant proteins was incubated with 5 μg of anti-Syk antibody (Cell Signaling Technology) overnight at 4°C. Immune complexes were collected by incubation with 25 μL protein A-Sepharose beads for 1 hour 30 minutes at 4°C. Immunoprecipitated complexes were washed 3 times with RIPA buffer, resuspended into Laemmli buffer, and analyzed by Western blot.

siRNA transfection assay

RL cells were transfected using Amaxa nucleofector kit V (Lonza). A total of 5 million cells were transfected with 200nM of SHP-1 siRNA duplex (5′GCAGGAGGUGAAGAACUUG3′) or siRNA control duplex (Eurogentec). Four hours after transfection, cells were seeded at 0.5×10^6 cells /mL in RPMI 10% FCS, and protein depletion was assessed 24 hours after transfection by Western blot analysis.

Calcium mobilization

A total of 3×10^6 cells were treated or not with RTX at 10 μg/mL for 16 hours. Cells were centrifuged and resuspended with RPMI 1% FCS at 1 million cells/mL. Staining with Indo-1 probe (Invitrogen) at 5 μg/mL was performed during 45 minutes at 37°C in the dark. Cells were then centrifuged 5 minutes at 1200*g*, washed with PBS, and resuspended in 500 μL PBS. Calcium flux was induced by BCR stimulation with anti-IgM antibody (10 μg/mL) or ionomycin (2μM) and analyzed on BD LSRII flow cytometer with BD FACSDiva 6.1.2 software.

Isolation of detergent-resistant membranes

DOHH2 cells (20×10^6) were washed with cold PBS and resuspended with 200 μL of D solution (150mM NaCl, 5mM dithiothreitol, 5mM ethylenediaminetetraacetic acid, 25mM Tris-HCl, pH 7.4, 1% Triton X-100; pH was adjusted to 7.4 and solution was supplemented with a cocktail of protease inhibitors) and left on ice for 30 minutes. A total of 400 μL of iodixanol (60%; Optiprep, Sigma-Aldrich) was added to the cell homogenate and overlayered on a step gradient consisting of 40%, 35%, 25%, 20%, and 0% iodixanol in the same buffer. Gradient was centrifuged during 4 hours at 33 400*g* using TST41.14 rotor. Five fractions were collected and analyzed by Western blot. Flotilin-1 (BD Biosciences) and Lyn (Santa Cruz Biotechnology) antibodies were used to assess raft fraction purity (fractions 1 and 2).

Isolation of detergent-free raft membranes

For cholesterol quantification, detergent-free raft membranes were isolated as described.[23] In brief, 10^8 cells were suspended in ice-cold 250mM

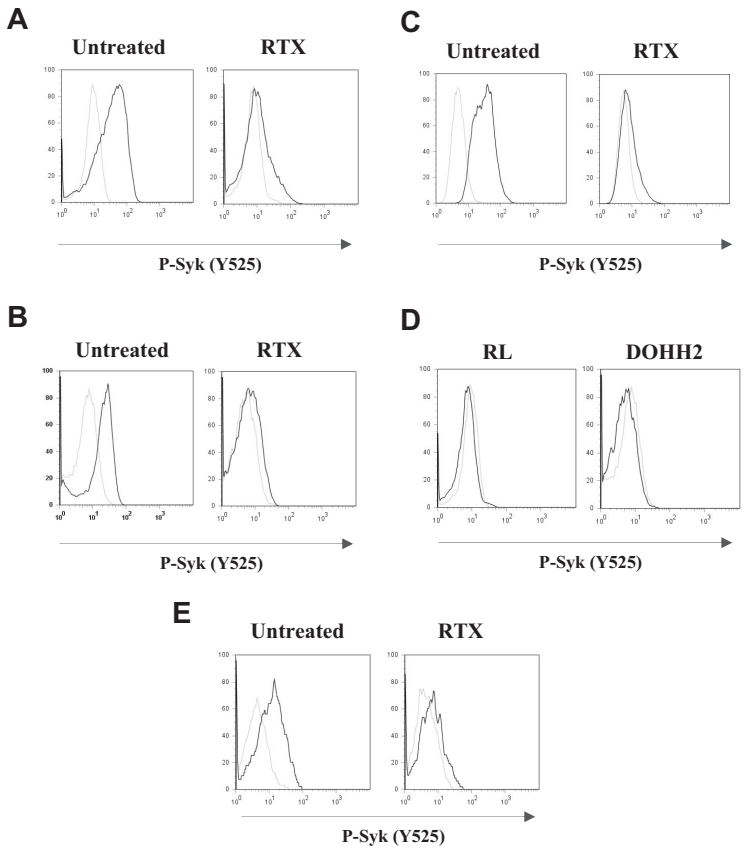

Figure 1. Effect of RTX on BCR activation in FL cell lines and normal B cells. RL (A,C) or DOHH2 (B) cells were incubated for 16 hours with 10 μg/mL of RTX or F(ab′)2 RTX, respectively, and then treated with anti-IgM or anti-IgG antibodies (10 μg/mL) during 5 minutes (A-B) or 2 hours (C). Nonstimulated and stimulated cells are represented by gray and black histograms, respectively. (D) RL or DOHH2 cells were treated with RTX or F(ab′)2 RTX, respectively (10 μg/mL, 16 hours). Untreated and treated cells with RTX are represented by gray and black histograms, respectively. (E) PBMCs isolated from healthy donors were incubated with F(ab′)2 RTX (10 μg/mL, 16 hours) and then treated with a mixture of anti-IgM/IgG antibody (10 μg/mL, 5 minutes). Nonstimulated and stimulated cells are represented by gray and black histograms, respectively. Syk phosphorylation on Y525 was measured by flow cytometry. Results are representative of at least 3 independent experiments.

sucrose, 1mM $CaCl_2$, 1mM $MgCl_2$, and 20mM Tris-HCl (pH 7.8) supplemented with protease inhibitor cocktail. Cell homogenate was sheared by repeated passage through needle and Dounce. Samples were centrifuged at 1000*g* for 10 minutes at 4°C, and the shearing/centrifugation steps were repeated on the cell pellets. Supernatants from each round were combined, mixed with an equal volume of 50% iodixanol, and overlayered with a step gradient consisting of 20% and 10% iodixanol. Samples were centrifuged for 90 minutes at 33 400*g* with TST41.14 rotor at 4°C. Twelve fractions were collected. Fractions from 2 to 5 were pooled, as well as fractions from 9 to 12 corresponding to the raft and nonraft fractions, respectively. Lipid content was analyzed as described in "Cholesterol quantification."

Cholesterol quantification

Lipids from raft and nonraft fractions (4 mL) were extracted according to Bligh and Dyer[24] in chloroform/methanol/water (2.5:2.5:2.1, v/v/v) in the presence of internal standards stigmasterol (2 μg). The dried lipid extract was sialylated in bis-(trimethylsilyl)trifluoroacetamide (1% TMSCl)-acetonitrile (1:1, v/v) overnight at room temperature.

Lipid extract (5 μL) was directly analyzed by gas-liquid chromatography on a 4890 Hewlett Packard system using a RESTEK RTX-50 fused silica capillary columns (30 m × 0.32 μm inner diameter, 0.1 μm film thickness). Oven temperature increased from 195°C to 310°C (12 minutes) 3.5°C per minute using hydrogen (0.5 bar) as carrier gas. Injector and detector were at 310°C and 340°C, respectively. Cholesterol was normalized in nanomoles per nanomole of total lipid phosphorus of the cell homogenate as described.[25]

Statistics

Data shown represent mean plus or minus SD. Significant differences were assessed by Student *t* test. *P* values less than .05 were considered statistically significant.

Results

Effect of RTX on BCR activation

In this study, we first evaluated the profile of BCR activation in both FL cell lines (RL and DOHH2) and gated $CD19^+$ normal B cells by measuring Syk phosphorylation level at site Y525. Several independent analyses of BCR activation kinetics have been performed (n = 15 for FL cell lines and n = 5 for normal B cells). As shown in Figure 1A-B,E, BCR stimulation resulted in increased Syk phosphorylation in both FL and normal B cells. However, FL cells displayed more rapid (1-5 minutes) and more sustained Syk phosphorylation (up to 3 hours), compared with stimulated normal B cells (data not shown).

In further experiments, RL or DOHH2 was pretreated with 10 μg/mL of RTX or F(ab′)2 RTX, respectively, and BCR stimulation was evaluated by Syk phosphorylation level (Y525) at 5 minutes (peak of BCR stimulation, data not shown). These experiments showed that, in BCR-stimulated cells, pretreatment with RTX seriously interfered with Syk phosphorylation in both RL and DOHH2 cells (Figure 1A,B, respectively). The time of preincubation with RTX appeared to be critical because we did not detect the inhibitory effect of RTX for DOHH2 and RL cell pretreatments shorter than 3 and 6 hours, respectively. Moreover, for both cell lines, prolonged time of RTX preincubation improved Syk inhibition level (data not shown). Thus, 16-hour incubation was used for further experiments. It is important to note that, in RTX-pretreated cells, BCR was unable to be activated even after prolonged stimulation (up to 2 hours), as shown in Figure 1C. Furthermore, we showed that RTX had no measurable effect on

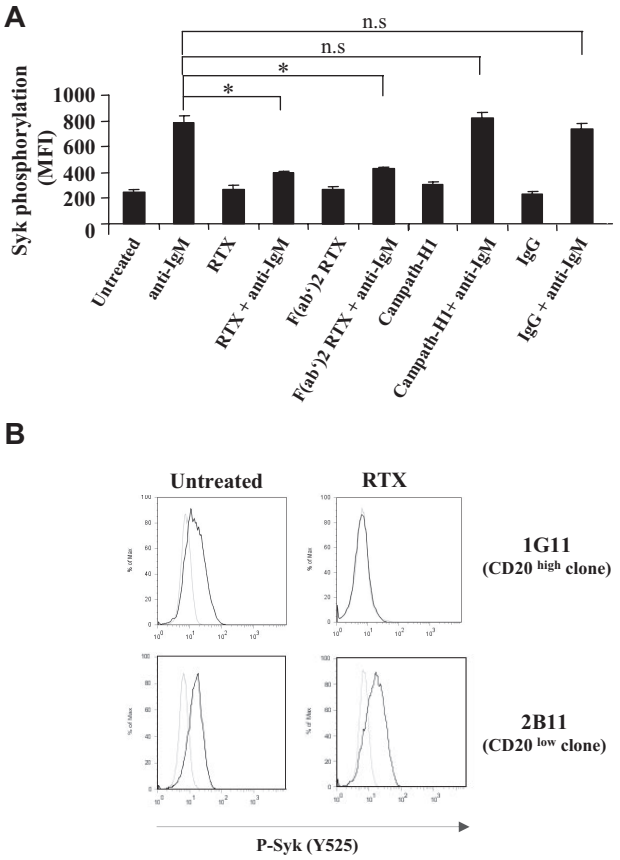

Figure 2. Influence of CD20 on RTX inhibitory effect. (A) BCR was stimulated in RL cells pretreated during 16 hours with 10 μg/mL of entire RTX, F(ab′)2 RTX, Campath-H1, or nonrelevant human IgG. Results represent Syk activation (Y525) expressed in MFI and are the mean of 3 independent experiments ± SD. *$P < .05$; n.s indicates not significant. (B) Syk activation (Y525) was evaluated on CD20 high (clone 1G11) and CD20 low (clone 2B11) expressing cells preincubated with RTX (10 μg/mL, 16 hours) and stimulated with anti-IgM (10 μg/mL, 5 minutes). Nonstimulated and stimulated cells are represented by gray and black histograms, respectively. Histograms are representative of 3 independent experiments.

constitutive Syk phosphorylation in nonstimulated RL and DOHH2 cells (Figure 1D) as we previously described.[9]

Based on these findings, we have asked whether RTX interfered with BCR signaling in non-neoplastic B cells. F(ab′)2 RTX did inhibit Y525 Syk phosphorylation in normal B cells activated by a mixture of anti-IgM and anti-IgG, as measured by cytometry analysis on $CD19^+$ gated cells issued from healthy donor PBMCs (Figure 1E).

Non-FL malignant cells, including mantle cell lymphoma (Granta) or large cell lymphoma (Daudi, DEAU, LIB), were also investigated. In these cells, BCR stimulation had low effect on Syk phosphorylation and RTX had no significant impact (data not shown), suggesting that the inhibitory effect of RTX correlated with the magnitude of BCR stimulation. These experiments suggested that RTX is a potent inhibitor of BCR signaling in normal and FL cells.

Role of CD20 in RTX-mediated BCR-signaling inhibition

We next investigated whether the effect of the antibody was mediated through CD20 engagement or related to Fcγ receptor (FcγR) through the binding of the RTX Fc moiety. As illustrated in Figure 2A, RTX F(ab′)2 was as efficient as unmodified RTX for inhibiting Syk phosphorylation at the Y525 site. Moreover, pretreatment of RL cells with either chimeric anti-CD52 (Mab-Campath-H1) or nonimmune IgG fraction was unable to interfere with Syk phosphorylation induced by BCR stimulation (Figure 2A). We further evaluated the influence of CD20 density on RTX inhibitory effect using 2 RL subclones expressing different CD20 level. The mean number of CD20 molecules per cell was 407 625 and 16 773 for 1G11 and 2B11 clone, respectively (data not shown). As shown in Figure 2B, RTX inhibited Syk phosphorylation in 1G11 but not in 2B11 clone. These results suggested that RTX acts through its F(ab′)2 moiety and that the level of CD20 expression is a limiting factor for inhibiting BCR activation.

Effect of RTX on Lyn activation in BCR-stimulated FL cell lines

The fact that RTX has no effect on Syk in nonstimulated FL cell lines (Figure 1D)[9] suggested that RTX acts upstream Syk. Lyn being the main regulator of Syk, we investigated whether RTX inhibited BCR-induced Lyn activation. We found that pretreatment with F(ab′)2 RTX reduced BCR-dependent Lyn phosphorylation in DOHH2 cells, as revealed by an immunoblot using anti–phospho-Src Y416. As visualized in Figure 3A, p56 Lyn isoform appeared more affected than its p53 isoform, whereas Lyn expression level remained unchanged.

The role of Lyn was substantiated by the inhibitory effect of RTX on Syk phosphorylation at both Y348 and Y352, 2 residues targeted by Lyn (Figure 3B). Based on these latter results, we hypothesized that RTX might prevent BCR/Syk association because Lyn facilitates the recruitment of Syk on ITAM-containing Igα. Using immunoprecipitation experiments, we confirmed that pretreatment with F(ab′)2 RTX abolished the Syk/Igα interaction (Figure 3C).

The mechanism by which RTX influences Lyn status in the context of BCR activation was then investigated. Based on the major Lyn-regulating role of SHP-1, we hypothesized that RTX acts through this tyrosine phosphatase. We thus evaluated the effect of SHP-1 inhibition by orthovanadate or SHP-1 depletion by siRNA on RTX inhibitory effect on Syk phosphorylation (Y525) in BCR-stimulated cells. As shown in Figure 3D, BCR signaling was unaffected in either SHP-1–inhibited or SHP-1–depleted FL cell lines, suggesting that SHP-1 played no role in RTX effect. These results suggested that Lyn is a target for RTX and contributes to its inhibition of BCR signaling.

Effect of RTX on other BCR-signaling components

In further experiments, we evaluated to which extent RTX interfered with downstream BCR-signaling components. It is well established that, on BCR stimulation, Syk activation induces stimulation of PLCγ2, Akt, and MAPK.[18] These phosphorylation events are key to propagate the BCR signaling and induce biologic functions of B lymphocytes (antigen presentation, survival, and proliferation). We found that, in FL cell lines, pretreatment with RTX for 16 hours strongly changed the global profile of tyrosine phosphorylation and dramatically reduced the $PLC\gamma_2$ activation (Figure 4A). Akt and ERK phosphorylation was also affected, although to a lesser extent. Furthermore, we observed that RTX also impacted on BCR-induced calcium fluxes, a well-described marker for BCR activation (Figure 4B). These results showed that, in accordance with its impact on Lyn and Syk activation, RTX does profoundly alter distal BCR-related signaling events.

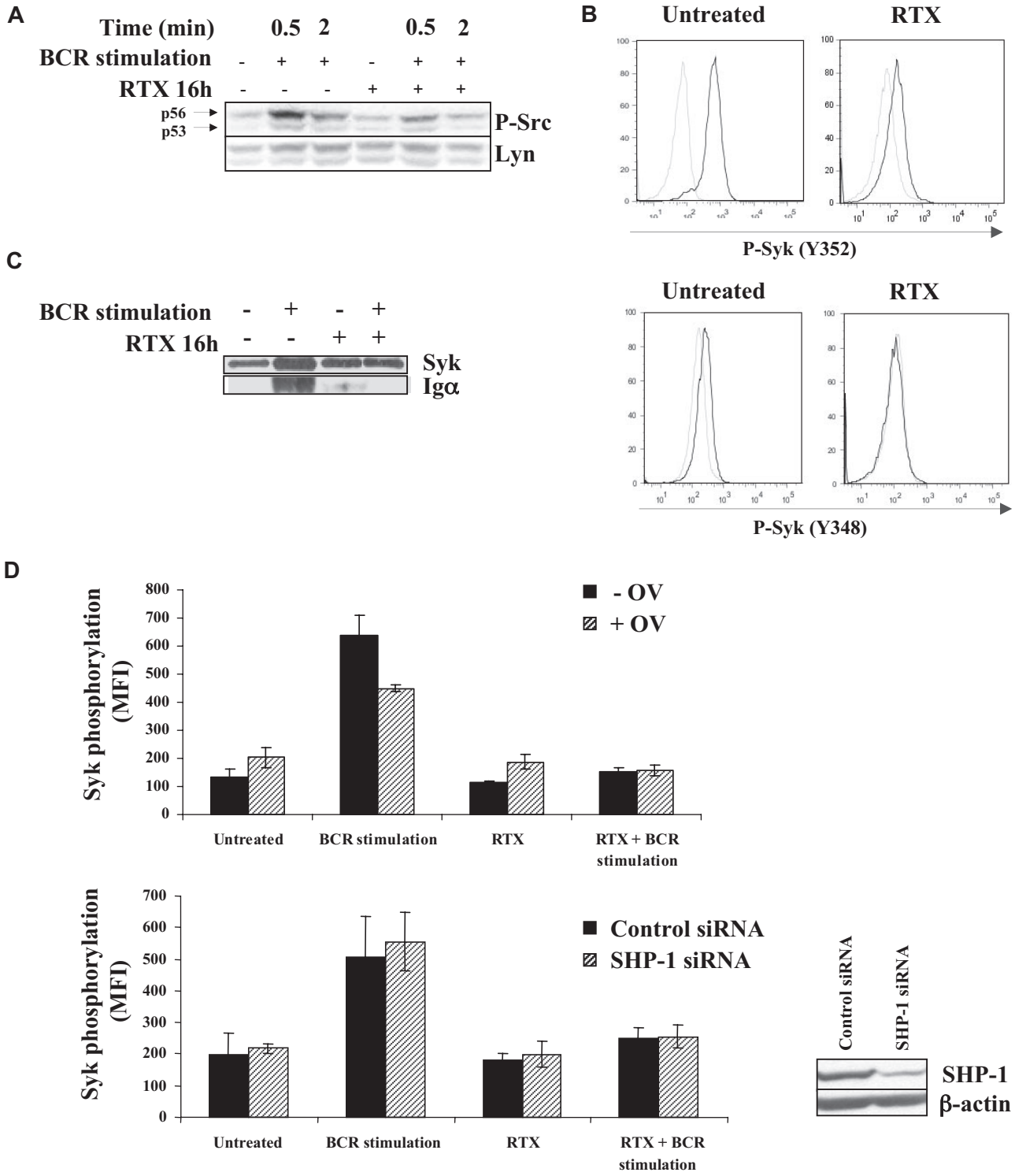

Figure 3. Effect of RTX on BCR-induced Lyn activation. (A) DOHH2 were preincubated with F(ab′)2 RTX (10 μg/mL, 16 hours) and then BCR was stimulated for the indicated times. Lyn activation was evaluated by an anti–phospho-Src antibody (Y416) revealing p53 and p56 Lyn isoforms. This result is representative of 3 independent experiments. (B) DOHH2 were preincubated with F(ab′)2 RTX (10 μg/mL, 16 hours) and stimulated with anti-IgG antibody (10 μg/mL, 5 minutes). Then, Lyn-dependent Syk phosphorylation was evaluated by flow cytometry using phycoerythrin-conjugated phospho-Syk (Y348 or Y352) antibodies. Nonstimulated and stimulated cells are represented by gray and black histograms, respectively, and are representative of 3 independent experiments. (C) Syk/BCR interaction was evaluated using DOHH2 preincubated with F(ab′)2 RTX (10 μg/mL, 16 hours) and stimulated or not with 10 μg/mL of anti-IgG antibody during 1 minute. BCR Igα associated with Syk was revealed by Western blot analysis. (D) SHP-1 was inhibited by 0.1mM sodium orthovanadate (OV) during 1 hour or depleted with SHP-1 siRNA. Then, FL cells were preincubated with RTX (16 hours, 10 μg/mL) and treated with anti-IgG (10 μg/mL, 5 minutes). Results represent Syk phosphorylation (Y525) expressed in MFI and are the mean of 3 independent experiments ± SD. (Inset) SHP-1 expression analyzed by Western blot in FL cell lines transfected by control or SHP-1 siRNA.

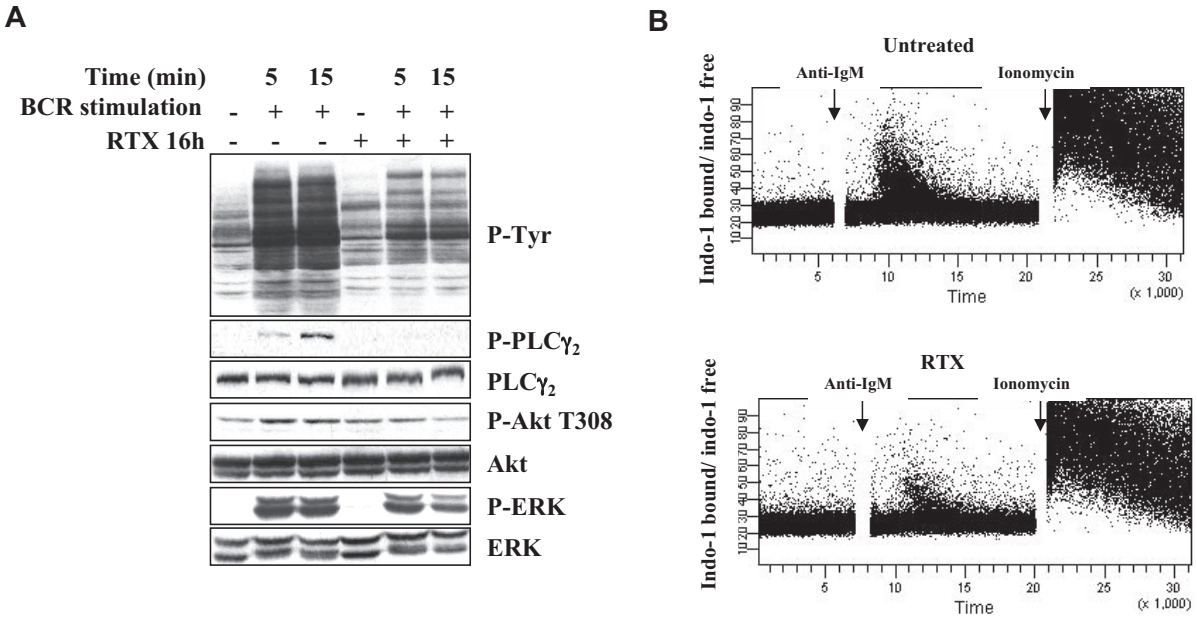

Figure 4. Effect of RTX on BCR-signaling components. (A) DOHH2 cells were preincubated with F(ab′)2 RTX (10 μg/mL, 16 hours) and stimulated with anti-IgG antibody (10 μg/mL, 5 or 15 minutes). Results are representative of 3 independent experiments. (B) Calcium mobilization was analyzed by flow cytometry. RL cells were preincubated with RTX (10 μg/mL, 16 hours), and calcium flux was stimulated by the addition of anti-IgM antibody (10 μg/mL). Ionomycin (2μM) was used as a positive control. Results are represented as ratio of indo-1 bound/indo-1 free and are representative of 3 independent experiments.

Effect of RTX on BCR translocation into raft and on membrane-associated cholesterol content

Previous studies have largely demonstrated that, on antigen stimulation, BCR translocates in part to membrane raft microdomains.[26,27] This event is now considered as one of the most proximal steps of BCR stimulation and critical for Lyn and Syk activation.[14,15] Based on the results obtained, we therefore speculated that RTX interfered with this important component of BCR activation. Thus, we evaluated BCR expression (Igα) in detergent-insoluble fractions after IgG cross-linking in F(ab′)2 RTX pretreated DOHH2 cells. As described in other B-cell models, Figure 5A shows that BCR activation resulted in the rapid (5 minutes) relocalization of a minor fraction of BCR into detergent-insoluble fractions (1 and 2), which contained Flotillin-1 and Lyn, 2 raft markers. However, RTX pretreatment totally inhibited the translocation of BCR into raft (Figure 5A).

This result suggested that pretreatment with RTX changed the composition of raft-contained lipids, cholesterol being the most representative. Moreover, cholesterol is essential for propagation of BCR signaling.[28,29] Thus, treatment with RTX could decrease the membrane-associated cholesterol. Paraformaldehyde-fixed cells stained with filipin, a naturally fluorescent tracker of cholesterol, revealed that RTX reduces the membrane cholesterol content (Figure 5B). To explore precisely whether RTX specifically affects the raft fraction, we performed chromatographic analysis of raft and non–raft-isolated fractions from RTX-treated cells. As shown in Figure 5C, RTX significantly decreased raft-associated cholesterol content in DOHH2 cells, compared with untreated cells. Non–raft-cholesterol content remained unchanged. Interestingly, treatment of FL cell lines with the cholesterol-depleting MβCD resulted in reduction of both cholesterol amount and BCR-activated Syk phosphorylation, compared with RTX-treated cells (Figure 5B,D). Altogether, these results showed that RTX alters BCR translocation into lipid raft microdomains, perhaps by decreasing raft-associated cholesterol.

Effect of RTX on BCR expression

As RTX seemed to affect BCR signaling by targeting proximal components of BCR activation, we hypothesized that RTX might directly target the BCR itself. Although speculative, this hypothesis was supported by a previous study showing that treatment with an anti-CD20 monoclonal antibody specific for another CD20 epitope than RTX significantly decreased the surface-associated IgM from both normal and malignant B cells.[30] Here, we show, for the first time, that prolonged exposure to RTX (16 hours) significantly reduced (at least 50%) the surface IgM and IgG from nonpermeabilized RL and DOHH2 cells, respectively (Figure 6A). IgM expression remained virtually unchanged in RTX-treated 2B11 low expressing CD20 RL subclone, whereas RTX exerts a potent effect on 1G11 (Figure 6B). This suggested that, as depicted for Syk inhibition, CD20 is a limiting parameter for the inhibitory effect of RTX on BCR expression. Reduction of BCR expression level was also found in experiments using cytometry with fixed and permeabilized cells (Figure 6Ci) or Western blot with whole cell extracts (Figure 6Cii), suggesting that RTX influenced the total amount of BCR and not only its surface expression.

This finding conflicted with Bourget's hypothetical model wherein anti-CD20 antibody reduced BCR expression by internalization, but rather argued for reduced BCR synthesis or its accelerated degradation. Proteasome-mediated BCR degradation has been demonstrated previously.[31,32] For this reason, we asked whether MG132-induced proteasome inhibition could prevent this RTX-reduced IgM expression and BCR signaling. Indeed, cotreatment with RTX and MG132 prevented RTX-induced IgM reduction in both total and surface-associated fractions (Figure 6D). Moreover, MG132 pretreatment restored BCR signaling as attested by normal Syk Y525 phosphorylation (Figure 6E). Similar results were observed with lactacystin, another proteasome inhibitor (data not shown). These results showed that CD20 binding by RTX reduced the expression of BCR by facilitating its degradation by proteasome.

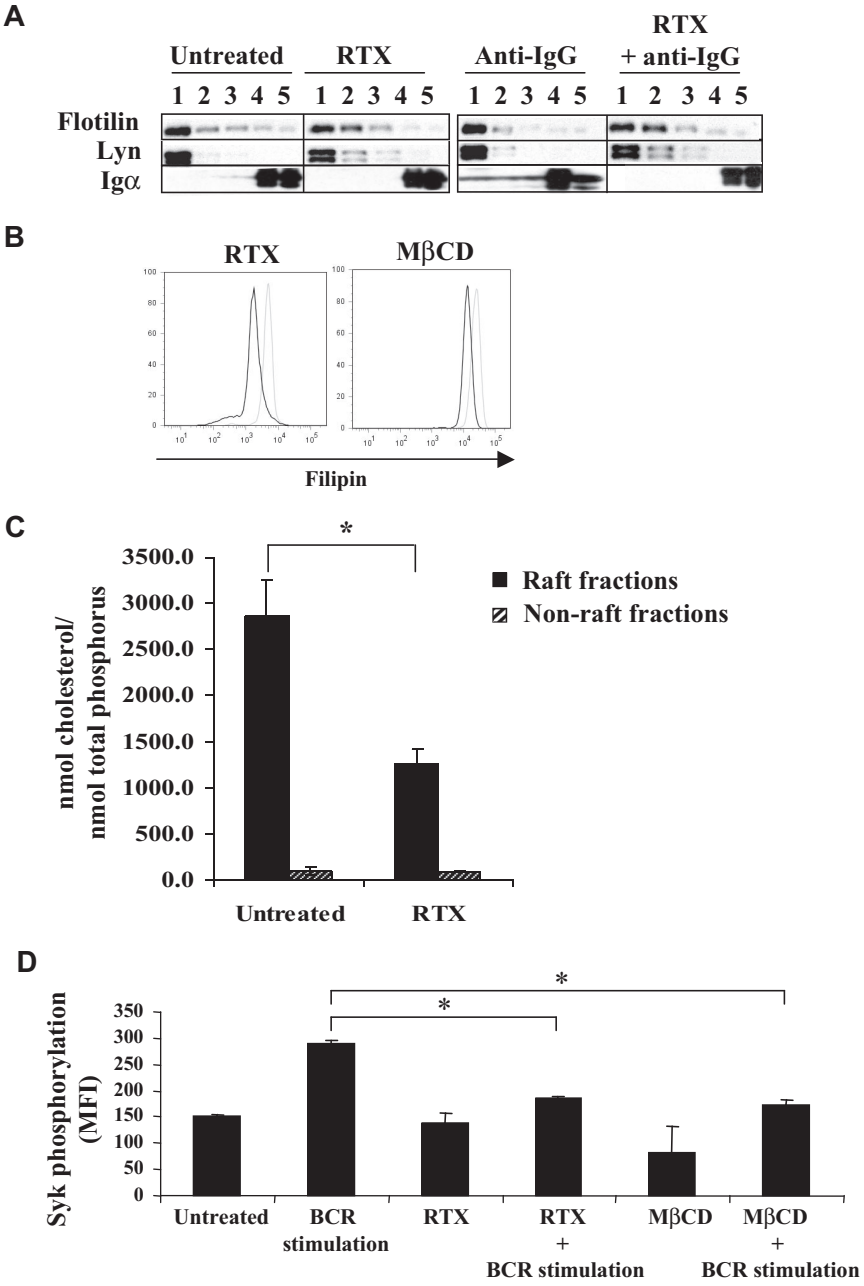

Figure 5. Effect of RTX on BCR translocation and on raft-associated cholesterol content. (A) DOHH2 cells were preincubated with F(ab′)2 RTX (10 μg/mL, 16 hours) and then stimulated with anti-IgG antibody (10 μg/mL, 5 minutes). Results are representative of 3 independent experiments. Vertical lines have been inserted to indicate a repositioned gel lane. (B) Cholesterol staining by filipin in RTX- or MβCD-treated and fixed RL cells (black histograms) compared with untreated and fixed cells (gray histograms). Results are representative of 3 independent experiments. (C) DOHH2 cells were treated with RTX (10 μg/mL, 16 hours), and cholesterol from raft and nonraft fractions was measured as described in "Methods." Histograms are the mean of 3 independent experiments ± SD. *$P < .005$ compared with untreated cells. (D) RL cells were preincubated with MβCD (5mM, 30 minutes), and then BCR was stimulated with anti-IgM antibody (10 μg/mL, 5 minutes). Histograms represent Syk phosphorylation (Y525) expressed in MFI and are the mean of 3 independent experiments ± SD. *$P < .005$ compared with BCR-stimulated cells.

Discussion

In this study, we demonstrate, for the first time, that RTX antagonizes the BCR-signaling cascade, from very proximal events such as BCR translocation to raft, to kinases activation and calcium flux. Most of these findings were obtained with transformed FL cell lines, which appear in our experience excellent models for investigating BCR signaling. Indeed, these cells displayed overreactive BCR activation, as previously described by Irish et al using fresh FL cells isolated from patients, compared with normal infiltrating tumor B cells.[21] The reason why FL cells displayed high magnitude BCR signaling, compared with other lymphomas as reported here, remains unknown but could be related to defective negative regulators, such as tyrosine phosphatase, or intrinsic abnormalities of BCR structure.[33,34] Moreover, FL cell lines, such as other immortalized cells, enabled us to carry out cell-consuming biochemistry and raft biology techniques, all hardly applicable to normal B cells. However, the physiologic relevance of our study is supported by the fact that RTX was also found to affect BCR signaling in normal B cells, as attested by Syk (Y525) phosphorylation, a hallmark of BCR activation.

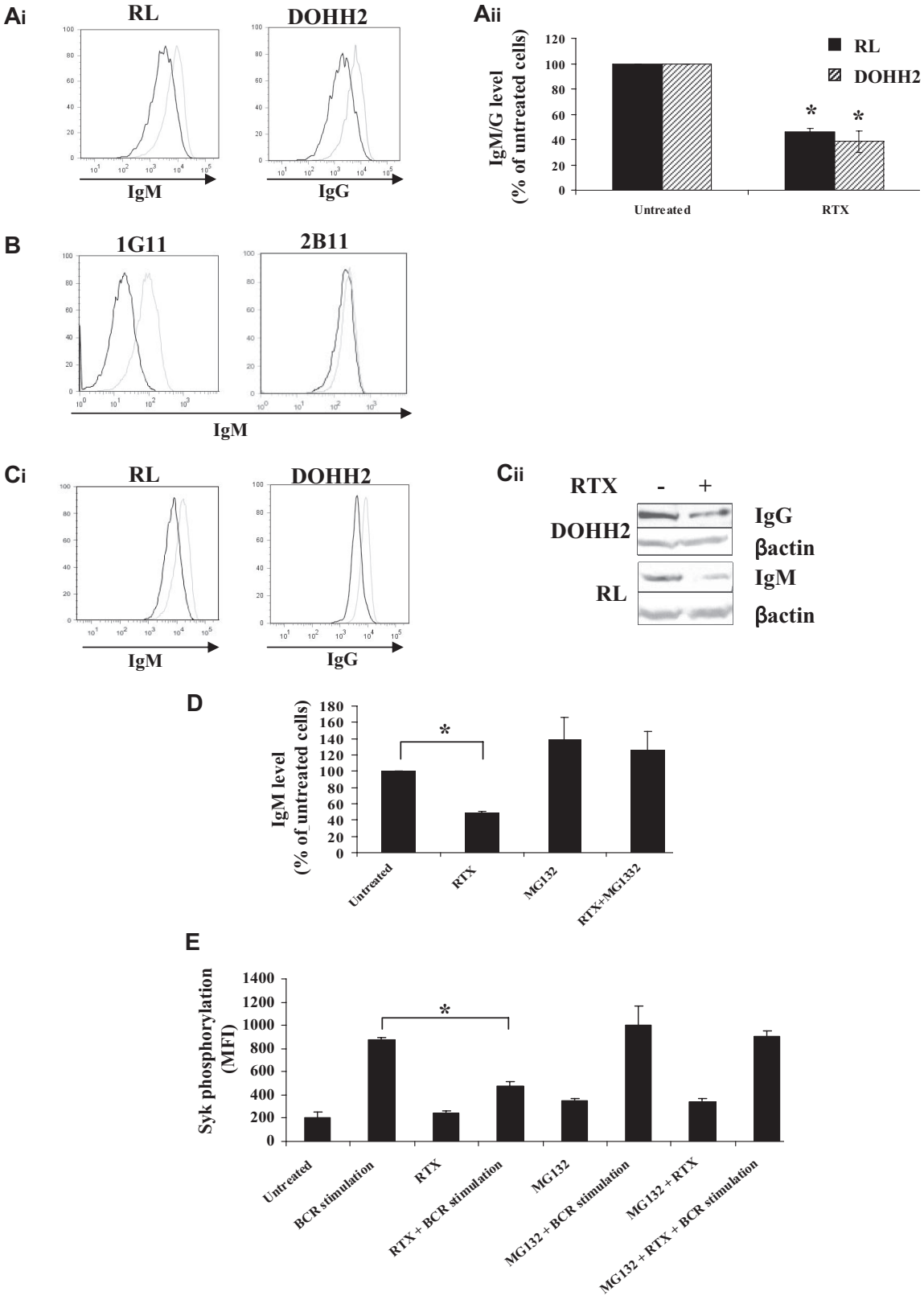

Figure 6. Effect of RTX on BCR expression and proteasome-mediated degradation. (A-B) BCR expression at the cell surface was evaluated by flow cytometry on fixed cells pretreated with RTX (10 μg/mL, 16 hours) and then stained with Cy5-conjugated anti-IgM antibody (RL, 1G11, 2B11) or Cy5-conjugated anti-IgG antibody (DOHH2). (Aii) Results are expressed as percentage of untreated cells and are the mean of 3 independent experiments ± SD. $P < .005$ compared with untreated cells. (C) Total BCR expression level was analyzed by flow cytometry with fixed and permeabilized FL cells (Ci) or by Western blot (Cii). (Ai,B,C1) Untreated and treated cells are represented by gray and black histograms, respectively. Histograms are representative of at least 3 independent experiments. (D) RL cells were cotreated with MG132 (10μM) and RTX (10 μg/mL) for 16 hours. BCR expression was analyzed as described in panel A. Results are expressed in percentage of untreated cells and are the mean of 3 independent experiments ± SD. *$P < .002$ compared with untreated cells. (E) RL cells were cotreated with MG132 (10μM) and RTX (10 μg/mL) for 16 hours. BCR was then stimulated with anti-IgM antibody (10 μg/mL, 5 minutes) and Syk phosphorylation (Y525) was evaluated by flow cytometry. Results are expressed in MFI and are the mean of 3 independent experiments ± SD. *$P < .002$ compared with BCR-stimulated cells.

The fact that RTX inhibits BCR in normal B cells might have functional consequences in terms of antibody production and, therefore, in risks of infection. However, it should be pointed out that patients routinely treated with RTX do not display reduced level of Ig and increased rate of infection.[35] However, it has been reported that prolonged RTX treatment could result in decreased serum IgM and reduced vaccinal response as well as a risk for infection in some vulnerable patients cotreated with other immunosuppressive drugs.[36] This effect so far was explained by the profound and sustained B-cell depletion. Our study offers another explanation through BCR inhibition.

RTX is now widely used for autoimmune disease, including arthritis and lupus erythematosus (LE).[2] The mechanisms by which RTX acts in the latter setting are not totally understood. However, B-cell depletion is generally thought to represent the main mechanism. However, BCR signaling is abnormal in patients with some autoimmune diseases, such as LE. In this disease, BCR-constitutive activation was proven and potentially related to defective FcγRIIB signaling or/and circulating B-cell stimulator.[37] Our study raises the possibility that, in LE, RTX also acts through BCR inhibition.

The fact that RTX inhibits BCR in malignant B cells may have some concerns in the context of hemato-oncology. Indeed, BCR plays a role in survival of malignant B cells, notably in some non-Hodgkin malignant lymphomas. Recently, Chen et al have described that a fraction of DLBCL patients displays a constitutive activation of Syk that was associated with high BCR density at the cell surface of these malignant cells.[20] The concept of so-called "tonic BCR" had a significant impact on the hematologist community thanks to the promise that new classes of Syk inhibitors become disposable for clinical use and would thus display unequivocally antilymphoma activity, both in vitro and in vivo.[20,38-40] The fact that RTX has no effect on Syk phosphorylation at Y525 in basal conditions invalidates the possibility that, in vivo, RTX acts directly as a simple "Syk inhibitor." However, if RTX treatment results in decreased BCR expression in clinical settings, as suggested by our in vitro experiments, it is conceivable that such modifications could prime malignant cells to apoptosis in "tonic BCR" DLBCL patients. This hypothesis may have significant implications with regards to the synergy between RTX and chemotherapy in DLBCL.

The mechanism by which RTX influences BCR signaling was examined. The fact that RTX had no effect on Syk status in basal conditions raised the possibility that RTX affects more proximal events; for example, it is conceivable that RTX influences BCR itself or its translocation into raft. Our study indicates that the 2 mechanisms are plausible and might coexist. Obviously, RTX treatment reduced expression of not only surface but also total Ig. This observation was not unprecedented as more than 10 years ago Bourget et al already reported reduction of surface Ig under treatment with another anti-CD20 monoclonal antibody.[30] This intriguing phenomenon has been neglected, and neither the mechanism nor the functional consequences have been examined for years. One of the most appealing implications of this observation is to establish a new link between CD20 and BCR. Indeed, previous studies have already documented that CD20 is physically and functionally linked to BCR. For example, CD20 and BCR colocalize and then rapidly dissociate at the cell surface before endocytosis of BCR,[41,42] whereas CD20 and BCR cooperate for activating calcium flux.[43] The mechanism by which RTX affects Ig expression has not been thoroughly investigated in our study. However, our results suggest a mechanism involving proteasome. Based on the literature, it is possible that RTX affects BCR degradation through distinct but coordinated mechanisms. First, RTX could regulate posttranslational events, such as glycosylation or ubiquitinylation, necessary for Ig folding and stability.[31] Second, RTX could interfere with the expression of chaperones, such as Bip and Calnexin, which are known to associate with Ig and target it to degradation.[44,45] Third, RTX may affect Ig-αβ subunit regulation, responsible for BCR assembly defect, and subsequent enhanced BCR IgM/G degradation.[46]

Our study also shows, for the first time, that treatment with RTX prevents BCR relocalization into raft. Depletion of raft-associated cholesterol and subsequent raft disorganization induced by RTX could be considered as sufficient to explain BCR-signaling cascade inhibition, as suggested by the previously documented potent inhibitory effect of MβCD on BCR signal propagation.[26] The mechanism by which RTX acts on cholesterol distribution or metabolism was beyond the scope of our paper. However, cholesterol depletion could be the result of RTX-induced membrane sphingolipid changes, including ceramide accumulation, as we previously described.[7] Indeed, this lipid messenger was shown to be able to interfere with both distribution and metabolism of cholesterol.[47,48]

In conclusion, our study provides several lines of evidence showing that RTX significantly interferes with BCR signaling by targeting proximal components of the BCR cascade, including decreased BCR expression and disturbances of BCR membrane dynamics, although the respective contribution of these 2 events, perhaps coordinated, should be determined. BCR inhibition might contribute to RTX immunosuppressive property.

Acknowledgments

The authors thank Catherine Trichard for technical assistance; Amandine Blanc for quantibrite analysis; Fatima-Ezzahra L'Faqihi-Olive for flow cytometry expertise (plateau de cytométrie en flux et tri cellulaire, IFR150, Toulouse, France); Véronique Roques and Séverine Viala (plateau de lipidomique, IFR150, Toulouse, France) for technical assistance; Emilie Laprévotte and Emilie-Fleur Gautier for reading the manuscript; and Loïc Dupré, Séverine Fruchon, Thierry Levade, Jany Ragab, Ashraf Ragab, and François Tercé for helpful discussions and invaluable advice.

This work was supported by Inserm and INCA (Pair Lymphome-Rituxop) and by l'Association pour la Recherche sur le Cancer (C.B.). S.K. is supported by le Ministère délégué à l'Enseignement Supérieur et à la Recherche.

Authorship

Contribution: S.K. conceived and designed the research plan, performed experiments, analyzed data, and drafted the manuscript; P.C., E.G., and A.Q.-M. performed experiments; J.B.-M. designed and performed lipid experiments; J.-J.F. contributed to the research plan and wrote the manuscript; and G.L. and C.B. designed the research plan, contributed to the interpretation, and wrote the manuscript.

Conflict-of-interest disclosure: The authors declare no competing financial interests.

Correspondence: Christine Bezombes, Inserm U563-CPTP, Bâtiment B, pavillon Lefebvre, Département d'Oncogenèse, Signalisation et Innovation Thérapeutique, CHU Purpan-BP3028, 31024 Toulouse Cedex 3, France; e-mail: christine.bezombes-cagnac@inserm.fr.

References

1. Molina A. A decade of rituximab: improving survival outcomes in non-Hodgkin's lymphoma. *Annu Rev Med.* 2008;59:237-250.
2. Gürcan HM, Keskin DB, Stern JN, Nitzberg MA, Shekhani H, Ahmed AR. A review of the current use of rituximab in autoimmune diseases. *Int Immunopharmacol.* 2009;9(1):10-25.
3. Smith MR. Rituximab (monoclonal anti-CD20 antibody): mechanisms of action and resistance. *Oncogene.* 2003;22(47):7359-7368.
4. Taylor RP, Lindorfer MA. Immunotherapeutic mechanisms of anti-CD20 monoclonal antibodies. *Curr Opin Immunol.* 2008;20(4):444-449.
5. Bonavida B. Rituximab-induced inhibition of antiapoptotic cell survival pathways: implications in chemo/immunoresistance, rituximab unresponsiveness, prognostic and novel therapeutic interventions. *Oncogene.* 2007;26(25):3629-3636.
6. Janas E, Priest R, Wilde JI, White JH, Malhotra R. Rituxan (anti-CD20 antibody)-induced translocation of CD20 into lipid rafts is crucial for calcium influx and apoptosis. *Clin Exp Immunol.* 2005; 139(3):439-446.
7. Bezombes C, Grazide S, Garret C, et al. Rituximab antiproliferative effect in B-lymphoma cells is associated with acid-sphingomyelinase activation in raft microdomains. *Blood.* 2004;104(4): 1166-1173.
8. Semac I, Palomba C, Kulangara K, et al. Anti -CD20 therapeutic antibody rituximab modifies the functional organization of rafts/microdomains of B lymphoma cells. *Cancer Res.* 2003;63(2): 534-540.
9. Leseux L, Laurent G, Laurent C, et al. PKC zeta mTOR pathway: a new target for rituximab therapy in follicular lymphoma. *Blood.* 2008; 111(1):285-291.
10. Alas S, Emmanouilides C, Bonavida B. Inhibition of interleukin 10 by rituximab results in down-regulation of bcl-2 and sensitization of B cell non-Hodgkin's lymphoma to apoptosis. *Clin Cancer Res.* 2001;7(3):709-723.
11. Jazirehi AR, Gan XH, De Vos S, Emmanouilides C, Bonavida B. Rituximab (anti-CD20) selectively modifies Bcl-xL and apoptosis protease activating factor-1 (Apaf-1) expression and sensitizes human non-Hodgkin's lymphoma B cell lines to paclitaxel-induced apoptosis. *Mol Cancer Ther.* 2003; 2(11):1183-1193.
12. Reth M. Antigen receptor tail clue. *Nature.* 1989; 338(6214):383-384.
13. Tolar P, Sohn HW, Pierce SK. Viewing the antigen-induced initiation of B cell activation in living cells. *Immunol Rev.* 2008;221:64-76.
14. Pierce SK. Lipid rafts and B cell activation. *Nat Rev Immunol.* 2002;2(2):96-105.
15. Gupta N, DeFranco AL. Lipid rafts and B cell signaling. *Semin Cell Dev Biol.* 2007;18(5):616-626.
16. Dal Porto JM, Gauld SB, Merrell KT, Mills D, Pugh-Bernard AE, Cambier J. B cell antigen receptor signaling 101. *Mol Immunol.* 2004;41(6): 599-613.
17. Keshvara LM, Isaacson CC, Yankee TM, Sarac R, Harrison ML, Geahlen RL. Syk- and Lyn-dependent phosphorylation of Syk on multiple tyrosines following B cell activation includes a site that negatively regulates signaling. *J Immunol.* 1998;161(10):5276-5283.
18. Campbell KS. Signal transduction from the B cell antigen-receptor. *Curr Opin Immunol.* 1999;11(3): 256-264.
19. Reth M, Brummer T. Feedback regulation of lymphocyte signaling. *Nat Rev Immunol.* 2004;4(4): 269-277.
20. Chen L, Monti S, Juszczynski P, et al. SYK-dependent tonic B cell receptor signaling is a rational treatment target in diffuse large B cell lymphoma. *Blood.* 2008;111(4):2230-2237.
21. Irish JM, Czerwinski DK, Nolan GP, Levy R. Altered B cell receptor signaling kinetics distinguish human follicular lymphoma B cells from tumor-infiltrating nonmalignant B cells. *Blood.* 2006; 108(9):3135-3142.
22. Vega MI, Huerta-Yepaz S, Garban H, Jazirehi A, Emmanouilides C, Bonavida B. Rituximab inhibits p38 MAPK activity in 2F7 B NHL and decreases IL-10 transcription: pivotal role of p38 MAPK in drug resistance. *Oncogene.* 2004;23(20):3530-3540.
23. Macdonald JL, Pike LJ. A simplified method for the preparation of detergent-free lipid rafts. *J Lipid Res.* 2005;46(5):1061-1067.
24. Bligh EG, Dyer WJ. A rapid method of total lipid extraction and purification. *Can J Biochem Physiol.* 1959;37:911-917.
25. Siakotos AN, Rouser G, Fleischer S. Phospholipid composition of human, bovine and frog myelin isolated on a large scale from brain and spinal cord. *Lipids.* 1969;4(3):239-242.
26. Cheng PC, Dykstra ML, Mitchell RN, Pierce SK. A role for lipid rafts in B cell antigen receptor signaling and antigen targeting. *J Exp Med.* 1999; 190(11):1549-1560.
27. Cheng PC, Brown BK, Song W, Pierce SK. Translocation of the B cell antigen receptor into lipid rafts reveals a novel step in signaling. *J Immunol.* 2001;166(6):3693-3701.
28. Blery M, Tze L, Miosge LA, Jun JE, Goodnow CC. Essential role of membrane cholesterol in accelerated BCR internalization and uncoupling from NF-kappa B in B cell clonal anergy. *J Exp Med.* 2006;203(7):1773-1783.
29. Karnell FG, Brezski RJ, King LB, Silverman MA, Monroe JG. Membrane cholesterol content accounts for developmental differences in surface B cell receptor compartmentalization and signaling. *J Biol Chem.* 2005;280(27):25621-25628.
30. Bourget I, Breittmayer JP, Grenier-Brossette N, Cousin JL. CD20 monoclonal antibodies down-regulate IgM at the surface of B cells. *Eur J Immunol.* 1993;23(3):768-771.
31. Ho SC, Chaudhuri S, Bachhawat A, McDonald K, Pillai S. Accelerated proteasomal degradation of membrane Ig heavy chains. *J Immunol.* 2000; 164(9):4713-4719.
32. Elkabetz Y, Kerem A, Tencer L, Winitz D, Kopito RR, Bar-Nun S. Immunoglobulin light chains dictate vesicular transport-dependent and -independent routes for IgM degradation by the ubiquitin-proteasome pathway. *J Biol Chem.* 2003;278(21): 18922-18929.
33. Hayslip J, Montero A. Tumor suppressor gene methylation in follicular lymphoma: a comprehensive review. *Mol Cancer.* 2006;5:44.
34. Radcliffe CM, Arnold JN, Suter DM, et al. Human follicular lymphoma cells contain oligomannose glycans in the antigen-binding site of the B cell receptor. *J Biol Chem.* 2007;282(10):7405-7415.
35. Walewski J, Kraszewska E, Mioduszewska O, et al. Rituximab (Mabthera, Rituxan) in patients with recurrent indolent lymphoma: evaluation of safety and efficacy in a multicenter study. *Med Oncol.* 2001;18(2):141-148.
36. van der Kolk LE, Baars JW, Prins MH, van Oers MH. Rituximab treatment results in impaired secondary humoral immune responsiveness. *Blood.* 2002;100(6):2257-2259.
37. Jenks SA, Sanz I. Altered B cell receptor signaling in human systemic lupus erythematosus. *Autoimmun Rev.* 2009;8(3):209-213.
38. Leseux L, Hamdi SM, Al Saati T, et al. Syk-dependent mTOR activation in follicular lymphoma cells. *Blood.* 2006;108(13):4156-4162.
39. Young RM, Hardy IR, Clarke RL, et al. Mouse models of non-Hodgkin lymphoma reveal Syk as an important therapeutic target. *Blood.* 2009; 113(11):2508-2516.
40. Friedberg JW, Sharman J, Schaefer-Cutillo J, et al. Fostamatinib disodium (FosD), an oral inhibitor of Syk, is well-tolerated and has significant clinical activity in diffuse large B cell lymphoma (DLBCL) and chronic lymphocytic leukemia (SLL/CLL). *Blood (ASH Annual Meeting Abstracts).* 2008;112:3.
41. Petrie RJ, Deans JP. Colocalization of the B cell receptor and CD20 followed by activation-dependent dissociation in distinct lipid rafts. *J Immunol.* 2002;169(6):2886-2891.
42. Polyak MJ, Li H, Shariat N, Deans JP. CD20 homo-oligomers physically associate with the B cell antigen receptor: dissociation upon receptor engagement and recruitment of phosphoproteins and calmodulin-binding proteins. *J Biol Chem.* 2008;283(27):18545-18552.
43. Walshe CA, Beers SA, French RR, et al. Induction of cytosolic calcium flux by CD20 is dependent upon B Cell antigen receptor signaling. *J Biol Chem.* 2008;283(25):16971-16984.
44. Hochstenbach F, David V, Watkins S, Brenner MB. Endoplasmic reticulum resident protein of 90 kilodaltons associates with the T- and B cell antigen receptors and major histocompatibility complex antigens during their assembly. *Proc Natl Acad Sci U S A.* 1992;89(10):4734-4738.
45. Foy SP, Matsuuchi L. Association of B lymphocyte antigen receptor polypeptides with multiple chaperone proteins. *Immunol Lett.* 2001;78(3): 149-160.
46. Dylke J, Lopes J, Dang-Lawson M, Machtaler S, Matsuuchi L. Role of the extracellular and transmembrane domain of Ig-alpha/beta in assembly of the B cell antigen receptor (BCR). *Immunol Lett.* 2007;112(1):47-57.
47. London M, London E. Ceramide selectively displaces cholesterol from ordered lipid domains (rafts): implications for lipid raft structure and function. *J Biol Chem.* 2004;279(11):9997-10004.
48. Subbaiah PV, Sowa JM, Singh DK. Sphingolipids and cellular cholesterol homeostasis: effect of ceramide on cholesterol trafficking and HMG CoA reductase activity. *Arch Biochem Biophys.* 2008; 474(1):32-38.